

# Nanoscale

Accepted Manuscript



This is an *Accepted Manuscript*, which has been through the Royal Society of Chemistry peer review process and has been accepted for publication.

*Accepted Manuscripts* are published online shortly after acceptance, before technical editing, formatting and proof reading. Using this free service, authors can make their results available to the community, in citable form, before we publish the edited article. We will replace this *Accepted Manuscript* with the edited and formatted *Advance Article* as soon as it is available.

You can find more information about *Accepted Manuscripts* in the [Information for Authors](#).

Please note that technical editing may introduce minor changes to the text and/or graphics, which may alter content. The journal's standard [Terms & Conditions](#) and the [Ethical guidelines](#) still apply. In no event shall the Royal Society of Chemistry be held responsible for any errors or omissions in this *Accepted Manuscript* or any consequences arising from the use of any information it contains.

Cite this: DOI: 10.1039/c0xx00000x

www.rsc.org/nanoscale

**COMMUNICATION**

## Well-oriented epitaxial gold nanotriangles and bowties on MoS<sub>2</sub> for surface-enhanced Raman scattering

Haiqing Zhou,<sup>‡ab</sup> Fang Yu,<sup>‡ab</sup> Chuan Fei Guo,<sup>a</sup> Zongpeng Wang,<sup>c</sup> Yucheng Lan,<sup>a</sup> Gang Wang,<sup>b</sup> Zheyu Fang,<sup>c</sup> Yuan Liu,<sup>a</sup> Shuo Chen,<sup>a</sup> Lianfeng Sun<sup>b,\*</sup> and Zhifeng Ren<sup>a,\*</sup>

<sup>5</sup> Received (in XXX, XXX) Xth XXXXXXXXX 20XX, Accepted Xth XXXXXXXXX 20XX

DOI: 10.1039/b000000x

We report on epitaxial growth of Au nanotriangles (AuNTs) and bowties consisting of opposing tip-to-tip AuNTs with a few-nanometer gap on n-layer MoS<sub>2</sub>. These AuNTs exhibit well-defined crystallographic orientation with the average size determined by MoS<sub>2</sub> thickness. Monolayer (1L) MoS<sub>2</sub> shows the 10 weakest coalescence, corroborating the layer-dependent interactions among Au and n-layer MoS<sub>2</sub>. High-resolution transmission electron microscopy characterization confirms the lattice directing of thin MoS<sub>2</sub> sheets on the AuNT formation with [111]<sub>Au</sub>||[001]<sub>MoS<sub>2</sub></sub> and <211><sub>Au</sub>||<210><sub>MoS<sub>2</sub></sub>. By introducing misfit dislocation arrays, the system with an 8.8% lattice misfit is stress-free. Especially, subwavelength-sized gold bowtie nanoantennas can be easily found on MoS<sub>2</sub> surface with a spacing gap down to 3 nm and a 15 density up to  $1.6 \times 10^{13} \text{ m}^{-2}$ . This technique is low cost, time-saving and free of impurities compared to the conventional lithography technologies. Meanwhile, the equilateral AuNTs can enhance Raman signals of thin MoS<sub>2</sub> sheets far stronger than that by ordinary gold films, indicating the potential use of AuNTs as SERS substrates for SERS applications.

### Introduction

20 Since the discovery of graphene in 2004,<sup>1</sup> considerable efforts have been devoted to two-dimensional layered materials.<sup>2-4</sup> With the thickness of a layered material reduced to nanoscale, the electronic, magnetic, optical and chemical properties may undergo remarkable changes depending on the number of layers, 25 which are obviously different from its bulk counterpart. For example, with reduced number of layers, size effects have been observed on surface diffusion of metal adatoms on graphene.<sup>5-7</sup> For n-layer MoS<sub>2</sub>, it has a tunable bandgap as the number of layers (thickness) decreases, and monolayer MoS<sub>2</sub> becomes a 30 direct band-gap semiconductor in contrast to few-layer or bulk MoS<sub>2</sub> with indirect bandgaps.<sup>8</sup> Especially, a single layer of MoS<sub>2</sub> can be divided into three weakly bonded S-Mo-S layers with one S layer at the surface through van der Waals force, which is suitable for metal adsorption and binding.<sup>9,10</sup> Furthermore, the 35 growth and anisotropic etching of MoS<sub>2</sub> single crystals usually exhibit triangular shapes.<sup>11-13</sup> Thus, due to its single crystalline nature, it is intuitive to imagine that two dimensional layered MoS<sub>2</sub> can be used as templates for the growth of single crystalline epilayers or crystallographically oriented 40 nanostructures. Although significant efforts have been devoted to investigating the electronic and optical properties of layered MoS<sub>2</sub> and its synthesis,<sup>8,11,14,15</sup> evaluating layered MoS<sub>2</sub>'s potential usefulness for epitaxial growth is still in its infancy.<sup>16</sup>

Nowadays controlled synthesis of AuNTs is of particular 45 interest because of their potential use in cancer hyperthermia, plasmonic nanoantennas,<sup>17</sup> and surface enhanced Raman

scattering (SERS),<sup>18</sup> etc. Usually, it is essential to assemble them on planar surfaces for many sensing and catalytic applications, which is achieved by post treatment after solution-phase 50 synthesis.<sup>19,20</sup> In this sense, it is highly desirable to realize the simultaneous growth and assembly of AuNTs without introducing any reagents in experiments. On the other hand, subwavelength-sized gold bowtie nanoantennas, consisting of two opposing tip-to-tip AuNTs separated by a small gap, has 55 attracted great attention due to its applications in SERS or fluorescence,<sup>21</sup> optical imaging and storage, molecular sensing,<sup>22</sup> etc. It is suggested that an extremely high electromagnetic field enhancement can be achieved within the gap and confined to the area near the gap due to the coupled plasmon resonance between 60 two AuNTs, which would serve as electromagnetically enhanced "hot spots" for SERS applications. The enhancement factors depend on the spacing gap<sup>23</sup>: The smaller the gap is, the stronger the enhancement is. However, there is no direct synthesis approach but only using expensive e-beam lithography (EBL) to 65 pattern gold bowties, with the spacing gap further limited by the system spatial resolution ( $\sim 8 \text{ nm}$ ).<sup>23</sup> The advent of two-dimensional layered MoS<sub>2</sub> may fill this gap, which would be an alternative template for growing AuNTs. In this paper, we demonstrate the direct growth and favorable orientation of 70 AuNTs on MoS<sub>2</sub> layers, and aim to unveil the effect of the number of MoS<sub>2</sub> layers on the AuNTs size and areal density. It is interesting to point out that upon heating the substrate, the as-deposited gold adatoms on MoS<sub>2</sub> tend to coalescent into ultrathin equilateral AuNTs, with the particle size and density tuned by 75 MoS<sub>2</sub> thickness. Few-layer MoS<sub>2</sub> shows better modulation on

particle shape than 1L MoS<sub>2</sub>, and AuNTs are surprisingly well-oriented on MoS<sub>2</sub> surface, resulting in the formation of gold bowtie structures with a high density up to  $1.6 \times 10^{13}$  counts/m<sup>2</sup> and interparticle spacing gap down to 3 nm. The AuNTs grow on MoS<sub>2</sub> with  $[111]_{\text{Au}} \parallel [001]_{\text{MoS}_2}$  and  $\langle 211 \rangle_{\text{Au}} \parallel \langle 210 \rangle_{\text{MoS}_2}$ , suggesting that the orientation of AuNTs originates from the lattice epitaxy between MoS<sub>2</sub> and AuNTs. These results indicate that although the MoS<sub>2</sub> interlayer interaction is usually thought to be weak and short ranged, it has profound effect on modulating the nucleation and growth of AuNTs on the MoS<sub>2</sub> basal plane. Meanwhile, strong Raman enhancements of AuNTs on MoS<sub>2</sub> are observed, which is much stronger than that based on ordinary gold film, indicating the potential use in SERS.

## Results and discussion

### Thickness determination of pristine n-layer MoS<sub>2</sub>

Ultrathin MoS<sub>2</sub> sheets were obtained by mechanical cleavage of bulk MoS<sub>2</sub>, and transferred onto 300 nm SiO<sub>2</sub>/Si substrates. The samples were first selected based on their color contrasts under an optical microscope. Fig. 1a and b show typical optical images of the as-prepared monolayer (1L), bilayer (2L), trilayer (3L), quadrilayer (4L) and multilayer (ML,  $n \geq 5$ ) MoS<sub>2</sub>, from which we can see the different color contrasts among MoS<sub>2</sub> flakes with different thickness. After selecting thin MoS<sub>2</sub> sheets, we have applied Raman and PL spectroscopy to further determine the number of MoS<sub>2</sub> layers (Fig. 1c and 1d). It is noteworthy that the frequency difference between two Raman  $A_{1g}$  and  $E'_{2g}$  modes (Fig. 1c) is distinctively different for different number of layers, which increases with the increase of MoS<sub>2</sub> layers. While in the PL spectra (Fig. 1d), the peak intensity of 1L at around 1.84 eV is much more prominent than other n-layer MoS<sub>2</sub>, which is due to the transition from indirect (few-layer) to direct (1L) band-gap semiconductor. The differences in Raman and PL spectra as a function of thickness are very consistent with previously reported results.

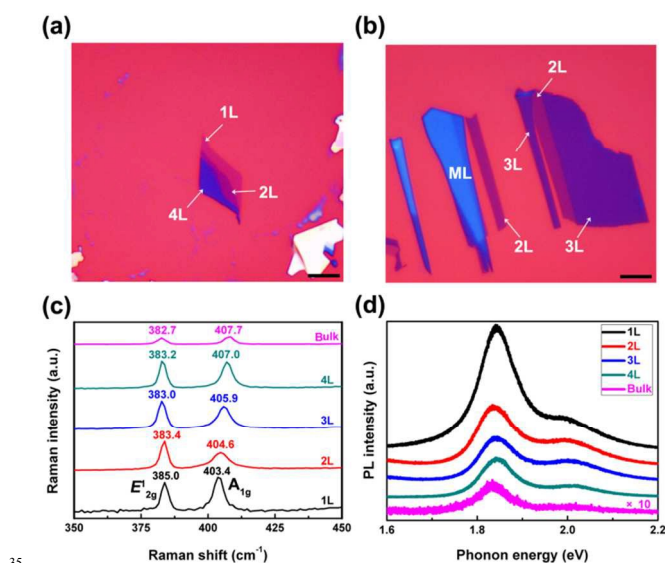


**Fig. 1** (a) A representative optical image of 1L, 2L and 4L MoS<sub>2</sub> transferred on silicon substrate. (b) An optical image showing the different color contrasts of 2L, 3L and ML MoS<sub>2</sub> on the substrate. Scale bar: 5  $\mu\text{m}$ . (c) and (d) Raman and PL spectra of n-layer

MoS<sub>2</sub> ( $n = 1, 2, 3, 4$  and bulk) excited by 514.5 nm, respectively.

### Epitaxial growth of AuNTs or gold bowties on MoS<sub>2</sub>

Although ultrathin MoS<sub>2</sub> sheets show hexagonal layered-lattice crystal structures, 1L MoS<sub>2</sub> is truly different from graphene in that it is composed of three atomic layers: A Mo layer sandwiched between two S layers. These would result in special properties on few-layer MoS<sub>2</sub> surface. To further demonstrate this point, we have thermally evaporated ultrathin gold onto pre-heated MoS<sub>2</sub> surface (ESI<sup>†</sup>), and investigated the effects of MoS<sub>2</sub> thickness on gold morphologies in details by using scanning electron microscopy (SEM).

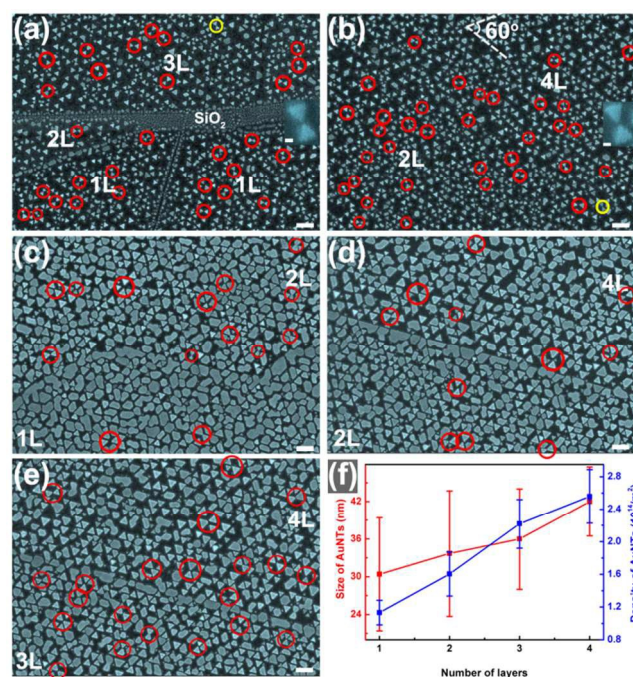


**Fig. 2** Typical SEM images showing the growth of ultrathin equilateral AuNTs on n-layer MoS<sub>2</sub> with controlled gold film thickness and substrate temperature. (a,b) 2.0 nm at 375  $^{\circ}\text{C}$ . The circles indicate the formation of gold bowties on MoS<sub>2</sub>, and the insets show the enlarged sizes of the yellow-marked bowties with 10 nm bar and false color. (c-e) 4.0 nm at 375  $^{\circ}\text{C}$ . (f) The statistical diagrams showing the edge length and density of AuNTs as a function of MoS<sub>2</sub> layers as shown in c-e. Scale bar for a-e: 100 nm.

By thermally depositing a thin gold film onto pre-heated MoS<sub>2</sub> surface, we find that the morphology of gold on MoS<sub>2</sub> is layer dependent (Fig. 2). On one hand, it is surprising to find that gold adatoms tend to nucleate and grow into AuNTs as shown in Fig. 2a and b, with the particle size modulated by MoS<sub>2</sub> thickness: The thicker the MoS<sub>2</sub> sheet is, the larger the size of AuNTs is (Fig. S1). By contrast, no AuNTs can be found on bare SiO<sub>2</sub>/Si substrate (Fig. 2a). These triangular structures are consistent with recently published results on the growth of MoS<sub>2</sub> single crystals by chemical vapor deposition (CVD) method, in which single grains tend to grow in triangular shape. The observed triangular shape (Fig. 2) may imply that a special direction of AuNTs is more stable when they are grown on MoS<sub>2</sub> surface, so as to ensure the smallest surface free energy during

growth. Once we deposit thicker gold film like 4.0 nm, some of the nanoparticles become irregular, so the effects of MoS<sub>2</sub> thickness on the shape of gold nanostructures become much more prominent (Fig. 2c-e): The AuNPs on 1L MoS<sub>2</sub> are mainly composed of irregular islands, while on thicker MoS<sub>2</sub>, like 2L, 3L or 4L, more AuNPs exhibit equilateral triangular shape, indicating that 1L MoS<sub>2</sub> is not so suitable for nanotriangle formation compared with other few-layer MoS<sub>2</sub> at the same condition. In particular, with the increase of MoS<sub>2</sub> thickness, the density of AuNTs becomes much higher, and the size gradually increases (Fig. 2c-e), making it evident that AuNTs are preferentially grown on few layer rather than on 1L MoS<sub>2</sub>, and the growth of triangular AuNPs is truly related to MoS<sub>2</sub> thickness. To account for the thickness dependence of gold morphologies on the number of MoS<sub>2</sub> layers, we need to consider the nucleation and growth of gold adatoms on MoS<sub>2</sub> surface, which is determined by the thickness-dependent surface diffusion coefficient and barrier caused by the interlayer interactions as in the situation of gold on graphene surface.<sup>5,7</sup> Meanwhile, it is apparent from the images (Fig. 2a-e) that the deposited Au atoms have the tendency to aggregate at MoS<sub>2</sub> edges or at terraced edges where MoS<sub>2</sub> flakes stacking together, which is probably attributed to the reason that Au atoms have larger binding energy with the edge Mo/S atoms than that at the central regions. For instance, the AuNPs are nearly connected with each other at the terraced edges between 2L and 4L (Fig. 2d), or 3L and 4L MoS<sub>2</sub> (Fig. 2e), indicating the aggregation of gold atoms at these border lines.

To the best of our knowledge, it is probably the first time gold bowties are directly synthesized on MoS<sub>2</sub> template without using the lithography method. As shown in Fig. 2a and b, it is worth mentioning that lots of bowtie structures (marked with red circles in Fig. 2a,b) consist of two nanotriangles with tip facing each other for gaps as small as 3 nm (The insets of Fig. 2a and b), which is much smaller than the reported value, and the relevant density can be up to  $1.6 \times 10^{13}$  counts/m<sup>2</sup>. Meanwhile, the gap in the gold bowties is in the range of 3-10 nm, and most of the gaps are around 4-6 nm (Fig. S2). Additionally, the size of gold bowties is closely related to the gold film thickness, and can be tuned through changing the film thickness (Fig. 2). With the increase of film thickness from 2 nm to 4 nm, the edge lengths of AuNTs range from ~20 nm to 40 nm, resulting in the formation of gold bowties with larger spatial size. Finally, we find that the areal density of gold bowties increases with the increase of the density of AuNTs.

#### 45 Lattice epitaxy between MoS<sub>2</sub> and AuNTs

To gain further insights into the effects of MoS<sub>2</sub> on the nucleation and growth of equilateral AuNTs, we carried out HRTEM observation to characterize the structural relationship between gold and MoS<sub>2</sub> (Fig. 3). The oriented nanotriangles are epitaxially grown on MoS<sub>2</sub>. Au has a face-centered cubic (fcc) crystal structure, which is six-fold-symmetric along the [111]-axis, while MoS<sub>2</sub> has a hexagonal structure and is also six-fold-symmetric along the [001]-axis. Although the lattice mismatch

$$f = \frac{d_{Au\{220\}} - d_{MoS_2\{110\}}}{d_{MoS_2\{110\}}} \quad (1)$$

between these two materials is large (8.8% between Au {220} and MoS<sub>2</sub> {110}, with *d*-spacing of 0.144 nm and 0.158 nm, respectively), the AuNTs can grow on MoS<sub>2</sub> surface by

introducing dislocation arrays with a pitch of ~1.68 nm to form stress-free interfaces. That is, dislocations appear every 11.6 Au {220} spacings or every 10.6 MoS<sub>2</sub> {110} spacings. Similar epitaxial growth has been reported in other systems with a large lattice misfit, like Zn/ZnO nanostructures.<sup>26</sup> Fig. 3a shows a representative HRTEM image of Au nanotriangles on MoS<sub>2</sub> with 1.68-nm-pitch Moiré fringes. Each Moiré fringe represents a misfit dislocation at the Au/MoS<sub>2</sub> interface. Fig. 3b exhibits the dislocations along the [211]-directions of Au or the [2 $\bar{1}$ 0]-directions of MoS<sub>2</sub>. Due to the six-fold symmetry of both materials, there are three dislocation arrays with an intersection angle of 120° at the Au/MoS<sub>2</sub> interface. Probably due to the fact that the HRTEM image was not exactly taken from the [001] zone axis of MoS<sub>2</sub>, we can only see one set of Moiré fringes perpendicular to one edge of the nanotriangle. However, we can find six-fold symmetry of the Moiré fringes by analyzing the Fourier transformation pattern of the TEM image, as shown in the yellow square in Fig. 3c. We also show a schematic (Fig. 3d) that explains the structural relationship between the AuNT and the underlying MoS<sub>2</sub>. And we predict that such a formation mechanism of AuNTs on MoS<sub>2</sub> may govern the growth of other metal with a fcc structure (e.g., Ag, Cu, Ni, and Al) or a hexagonal structure (e.g., Zn), enabling much wider applications. However, for different metals the distance between neighboring dislocations differs as a result of changed extent of lattice misfit.

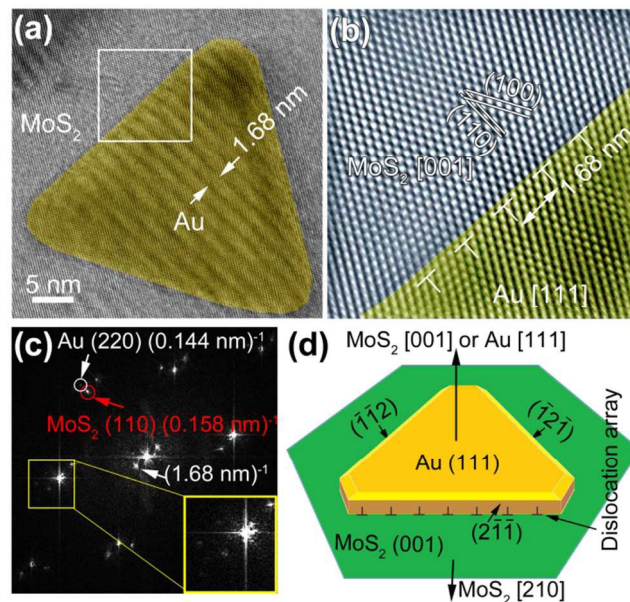


**Fig. 3** Epitaxial growth of Au nanotriangles. (a) HRTEM image of a AuNT on MoS<sub>2</sub>. (b) Fourier filtered image of the white square in panel (a), showing a dislocation array with a spacing of 1.68 nm at the boundary of the Au triangle. (c) Fourier transformation pattern of the Au triangle, indicating that Au triangles are grown on MoS<sub>2</sub> with {220}<sub>Au</sub>||{110}<sub>MoS<sub>2</sub></sub>. The diffraction spots in the yellow square exhibit a six-fold symmetry of the dislocations. (d) Schematic of the structural relationship between Au and MoS<sub>2</sub>. Note that there are three dislocation arrays that are perpendicular to the (211), (121) and (112) facets of the AuNT, respectively.

#### 95 Highly-Improved Raman enhancement

To search for the possible applications of this kind of MoS<sub>2</sub>-based composites, we have used Raman spectroscopy to investigate the SERS properties of well-oriented AuNTs (Fig. 4). The micro-Raman spectroscopy (Renishaw inVia Raman Spectroscopy) experiments were performed under ambient conditions with a 785 nm (1.58 eV) laser. All the spectra were collected under the same ambient conditions (laser power, exposure time, etc.). As shown in Fig. 4a and b, it is clearly seen that Raman signals of as-fabricated MoS<sub>2</sub> samples are almost undetectable at 785 nm laser excitation. When a 2 nm gold film is deposited onto MoS<sub>2</sub> surface at room temperature, we can detect the Raman signal with the Raman peaks appearing clearly, however, the signal is relatively weak. By contrast, if n-layer MoS<sub>2</sub> is fully covered by AuNTs prepared by our method, the Raman signals of 1L or 2L MoS<sub>2</sub> are greatly enhanced, indicating that triangular AuNTs can efficiently enhance Raman scattering of n-layer MoS<sub>2</sub> compared with ordinary gold particles. This could be attributed to the sharp corners in a nanotriangle, where electromagnetic fields are concentrated into “hot-spots”, thus resulting in strong Raman enhancements on the Raman signals of MoS<sub>2</sub>.<sup>21,27</sup> In order to figure out the physical origins, we have carried out theoretical simulations (ESI†). Indeed, according to the electromagnetic field contour (Fig. 4c), there is a very strong field enhancement at the sharp edges of a nanotriangle or a bowtie structure. Especially, by examining the relevant extinction spectrum, we can note that there is a strong in-plane dipole plasmon resonance at 785 nm in an AuNT (black in Fig. 4d), while for gold bowties, their extinction spectra also show prominent resonant peaks close to 785 nm (red in Fig. 4d, Fig. S4, ESI†), suggesting the contribution of single AuNT or bowties to the Raman enhancement arising from the coupled surface plasmon resonance absorption. These results would further boost the application of MoS<sub>2</sub>-based metal composites in possibly SERS.

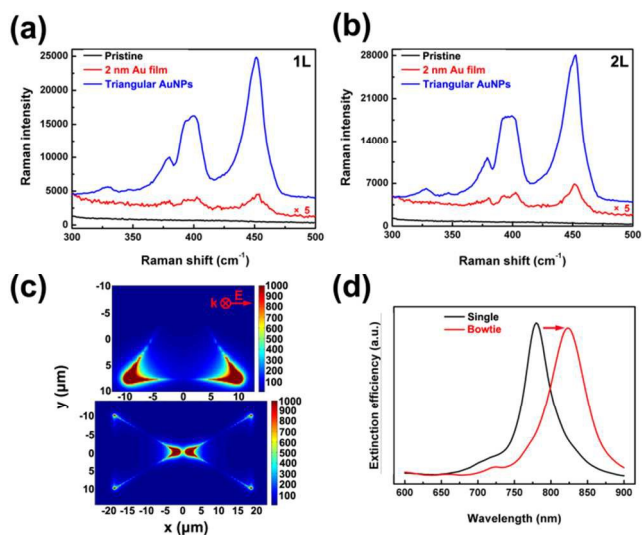


**Fig. 4** The comparison among the Raman spectra of original MoS<sub>2</sub>, gold film-deposited on MoS<sub>2</sub> and ultrathin AuNTs-decorated on 1L (a) and 2L (b) MoS<sub>2</sub> excited by a 785 nm laser. (c) The electromagnetic field enhancement contour external to an individual AuNT and bowtie with a 2 nm thickness and 20 nm edge length at a 785 nm laser excitation. (d) The calculated extinction spectrum of a nanotriangle and relevant bowtie

structure with a spacing gap of 3 nm.

## Conclusions

In summary, we report here the nucleation and growth of equilateral triangular AuNPs on layered MoS<sub>2</sub> with well-defined crystallographic orientation, and an average size controlled by MoS<sub>2</sub> thickness, suggesting thickness-dependent interactions and the epitaxial growth of Au on n-layer MoS<sub>2</sub>. Our technique is of great potential for direct synthesis of gold bowtie nanoantennas where two AuNTs opposing tip to tip with the gap as small as 3 nm, which is far below the spatial resolution of e-beam lithography (~ 8 nm). Especially, these well-oriented AuNTs exhibit excellent Raman enhancing effects, indicating the potential application of AuNTs for molecule detection.

## Acknowledgements

This project was partially supported by National Natural Science Foundation of China (Grant Nos. 10774032, 51472057, 61422501 and 11374023), the National Basic Research Program of China (973 Program) (Grant no. 2015CB932400), Beijing Natural Science Foundation (Grant no. L140007), and partially by US Defense Threatening Reduction Agency (DTRA) under grant FA 7000-13-1-0001.

## Notes and references

<sup>a</sup>Department of Physics and TcSUH, University of Houston, Houston, TX 77204, USA. E-mail: zren@uh.edu

<sup>b</sup>National Center for Nanoscience and Technology, Beijing 100190, China. E-mail: slf@nanocr.cn

<sup>c</sup>School of Physics, State Key Lab for Mesoscopic Physics, Peking University and Collaborative Innovation Center of Quantum Matter, Beijing, China.

<sup>†</sup>Electronic Supplementary Information (ESI) available: The experimental details and characterization data. See DOI: 10.1039/b000000x/.

<sup>‡</sup>These authors contributed equally to this work.

- 1 K. S. Novoselov, A. K. Geim, S. V. Morozov, D. Jiang, Y. Zhang, S. V. Dubonos, I. V. Grigorieva and A. A. Firsov, *Science*, 2004, **306**, 666-669.
- 2 K. S. Novoselov, D. Jiang, F. Schedin, T. J. Booth, V. V. Khotkevich, S. V. Morozov, A. K. Geim, *Proc. Natl Acad. Sci. USA* 2005, **102**, 10451-10453.
- 3 Q. H. Wang, K. Kalantar-Zadeh, A. Kis, J. N. Coleman, M. S. Strano, *Nat. Nanotechnol.* 2012, **7**, 699-712.
- 4 Z. Liu, L. Song, S. Z. Zhao, J. Q. Huang, L. L. Ma, J. N. Zhang, J. Lou, P. M. Ajayan, *Nano Lett.* 2011, **11**, 2032-2037.
- 5 H. Q. Zhou, C. Y. Qiu, Z. Liu, H. C. Yang, L. J. Hu, J. Liu, H. F. Yang, C. Z. Gu, L. F. Sun, *J. Am. Chem. Soc.* 2010, **132**, 944-946.
- 6 Z. T. Luo, L. A. Somers, Y. P. Dan, T. Ly, N. J. Kybert, E. J. Mele, et al. *Nano Lett.* 2010, **10**, 777-781.
- 7 H. Q. Zhou, F. Yu, M. J. Chen, C. Y. Qiu, H. C. Yang, G. Wang, T. Yu, L. F. Sun, *Carbon* 2013, **52**, 379-387.
- 8 K. F. Mak, C. Lee, J. Hone, J. Shan, T. F. Heinz, *Phys. Rev. Lett.* 2010, **105**, 136805.
- 9 J. R. Lince, D. J. Carre, P. D. Fleischauer, *Phys. Rev. B* 1987, **36**, 1647.
- 10 T. S. Sreeprasad, P. Nguyen, N. Kim, V. Berry, *Nano Lett.* 2013, **13**, 4434.

- 11 S. Najmaei, Z. Liu, W. Zhou, X. L. Zou, G. Shi, S. D. Lei, B. I. Yakobson, J. C. Idrobo, P. M. Ajayan, J. Lou, *Nat. Mater.* 2013, **12**, 754-759.
- 12 H. Q. Zhou, F. Yu, Y. Y. Liu, X. L. Zou, C. X. Cong, C. Y. Qiu, T. Yu, Z. Yan, X. N. Shen, L. F. Sun, B. I. Yakobson, J. M. Tour, *Nano Res.* 2013, **6**, 703-711.
- 13 S. Helveg, J. V. Lauritsen, E. Lægsgaard, I. Stensgaard, J. K. Nørskov, B. S. Clausen, H. Topsøe, F. Besenbacher, *Phys. Rev. Lett.* 2000, **84**, 951.
- 14 B. Radisavljevic, A. Radenovic, J. Brivio, V. Giacometti, A. Kis, *Nat. Nanotechnol.* 2011, **6**, 147-150.
- 15 A. Splendiani, L. Sun, Y. B. Zhang, T. S. Li, J. Kim, C. Y. Chim, G. Galli, F. Wang, *Nano Lett.* 2010, **10**, 1271-1275.
- 16 T. S. Sreeprasad, P. Nguyen, N. Kim, V. Berry, *Nano Lett.* 2013, **13**, 4434-4441.
- 17 M. W. Knight, H. Sobhani, P. Nordlander, N. J. Halas, *Science* 2011, **332**, 702-704.
- 18 L. Scarabelli, M. Coronado-Puchau, J. J. Giner-Casares, J. Langer, L. M. Liz-Marzán, *ACS Nano* 2014, **8**, 5833-5842.
- 19 D. A. Walker, K. P. Browne, B. Kowalczyk, B. A. Grzybowski, *Angew. Chem. Int. Ed.* 2010, **49**, 6760-6763.
- 20 P. R. Sajanlal, T. Pradeep, *Adv. Mater.* 2008, **20**, 980-983.
- 21 A. Kinkhabwala, Z. F. Yu, S. H. Fan, Y. Avlasevich, K. Müllen, W. E. Moerner, *Nat. Photonics* 2009, **3**, 654-657.
- 22 N. Liu, M. L. Tang, M. Hentschel, H. Giessen, A. P. Alivisatos, *Nat. Mater.* 2011, **10**, 631-636.
- 23 N. A. Hatab, C. Hsueh, A. Gaddis, S. Retterer, J. H. Li, G. Eres, Z. T. Zhang, B. H. Gu, *Nano Lett.* 2010, **10**, 4952-4955.
- 24 C. G. Lee, H. G. Yan, L. E. Brus, T. F. Heinz, J. Hone, S. Ryu, *ACS Nano* 2010, **4**, 2695-2700.
- 25 A. M. van der Zande, P. Y. Huang, D. A. Chenet, T. C. Berkelbach, Y. M. You, G. H. Lee, T. F. Heinz, D. R. Reichman, D. A. Muller, J. C. Hone, *Nat. Mater.* 2013, **12**, 554-561.
- 26 C. F. Guo, Y. Wang, P. Jiang, S. Cao, J. Miao, Z. Zhang, Q. Liu, *Nanotechnology* 2008, **19**, 445710.
- 27 P. J. Schuck, D. P. Fromm, A. Sundaramurthy, G. S. Kino, W. E. Moerner, *Phys. Rev. Lett.* 2005, **94**, 017402.

### The table of contents entry

Due to the lattice epitaxy between MoS<sub>2</sub> and gold nanotriangles (AuNTs), ultrathin equilateral AuNTs and gold bowties can be epitaxially grown on two-dimensional MoS<sub>2</sub> sheets with favorable orientation, which further exhibit excellent Raman enhancements on Raman signals of underlying MoS<sub>2</sub>.

### TOC figure

